Micromagnetic Characteristics of Transverse Diffuse Domain Boundaries in Permalloy Thin Films

MARK H. KRYDER AND FLOYD B. HUMPHREY, MEMBER, IEEE

Abstract—Transverse domain boundaries propagating in the longitudinal direction at speeds one to three orders of magnitude faster than normal domain walls are responsible for most of the lower speed reversals in magnetic thin films. Using a 10-ns exposure time Kerr magnetooptic camera, these boundaries have been photographed for a variety of applied fields in several films with thicknesses ranging from 500 to 3500 Å. High-magnification photographs of the boundary transition region reveal that the boundaries consist of small isolated areas of reversed and partially reversed magnetization in a nonreversed background. Propagation occurs by the nucleation of additional small areas of reverse magnetization within and ahead of the transition region. In a given film the width of the transition region increases as the applied field is increased. By approximating the divergence of the magnetization at the boundary as a line charge, a model has been derived which predicts the boundary width W to be

$$W = \frac{8M_s t}{H_n} \frac{1}{(1 - H/H_n)}$$

where M_s is the saturation magnetization and H is the applied field. The nucleation threshold H_n is the threshold at which nucleation is observed over all the film. The experimental data fit this predicted dependence quite well. The rapid increase in width of the transition region with applied field is correlated with a rapid nonlinear increase in the velocity of propagation.

Introduction

USING A 10-ns exposure time Kerr magnetooptic camera [1], Kryder and Humphrey have previously reported [2], [3] that a primary mechanism of magnetic flux reversal in Permalloy thin films is the propagation of diffuse domain boundaries. The boundaries were found to be quite different from quasi-static domain walls. Instead of lying parallel to the easy axis and propagating transversely to it, the boundaries lie along the transverse direction and propagate longitudinally. Furthermore, boundary widths and velocities were reported to be several orders of magnitude greater than those of normal domain walls. In this paper data on the dynamic equilibrium structure, width, and velocity of the boundaries are discussed and related to simple models.

The films used in this study were vacuum evaporated from melts of 83 percent Ni and 17 percent Fe onto glass substrates at 200–250°C in a vacuum of 10^{-6} torr in the presence of a uniform magnetic field in the plane of the substrate. The anisotropy field H_k, coercive force H_c, dispersion α_{90}, and film thickness t of each film were measured using a 20-Hz hysteresis loop tracer and are listed in Table I. The films were coated with 330 Å of SiO for enhancement of the Kerr effect.

TABLE I
FILM CHARACTERISTICS

Film	H_k(Oe)	H_c(Oe)	t(Å)	H_n(Oe)	α_{90}
A	2.9	2.4	500	5.0	2.0°
B	3.6	1.7	960	5.2	1.7°
C	3.3	1.4	1700	4.9	3.0°
D	3.2	0.57	3500	4.4	5.0°

Kerr Photographs

Kerr magnetooptic photographs of three characteristic dynamic states in ferromagnetic thin films are shown in Fig. 1. The 1-cm diameter circular thin films appear elliptical because the camera is oriented at 60° to the normal. In all figures the easy anisotropy axis is vertical. In Fig. 1(a) and (b), the films are reversing mainly by the growth of domains in the longitudinal (easy-axis) direction. In Fig. 1(c), nucleation has occurred over the entire film. Examples of complete reversals involving magnetization states like those in Figs. 1(a) (b), and (c) can can be found in [2] and [4]. It was shown elsewhere [4] that even during reversals involving pulse fields barely sufficient to drive a film to remanence (as in Fig. 1(a), where film B has 2.5 Oe applied), the longitudinal propagation of the diffuse boundaries at the end of the domains is much faster than the transverse propagation of the longitudinal domain walls. In addition, the boundary width is quite wide (>50 μm) in comparison to a normal domain wall (4000 Å) [5]. The boundary transition region of Fig. 1(a) is shown at high magnification in Fig. 2(a). In this case the transition region consists of many reversed and partially reversed areas extending from the totally reversed region at the top into the nonreversed region at the bottom. The poor definition of these extended areas indicates that there is not a sharp wall defining them, but that the magnetization gradually turns from the nonreversed to reversed state.

The areas of reversed and partially reversed magnetization in the transition region do not extend from the reversed

Manuscript received March 4, 1971; revised May 10, 1971. Paper 25.7, presented at the 1971 INTERMAG Conference, Denver, Colo., April 13–16. This work was supported by the Burroughs Corporation and the NSF.

The authors are with the California Institute of Technology, Pasadena, Calif. 91109

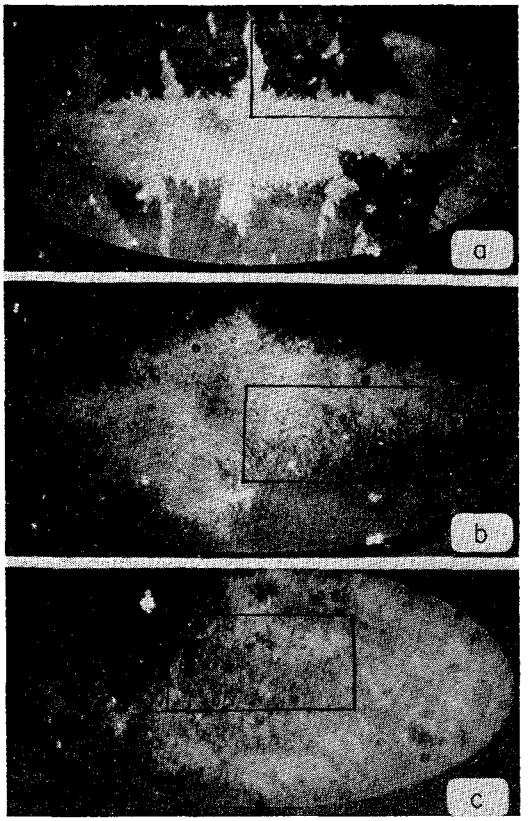

Fig. 1. (a) Film B in process of flux reversal by diffuse boundary propagation 8 μs after application of 2.5-Oe longitudinal pulse field. (b) Film B in process of flux reversal by diffuse boundary propagation 250 ns after application of 4.7-Oe longitudinal pulse field. (c) Film A in process of flux reversal by nucleation of partially reversed regions 250 ns after application of 5.2-Oe longitudinal pulse field.

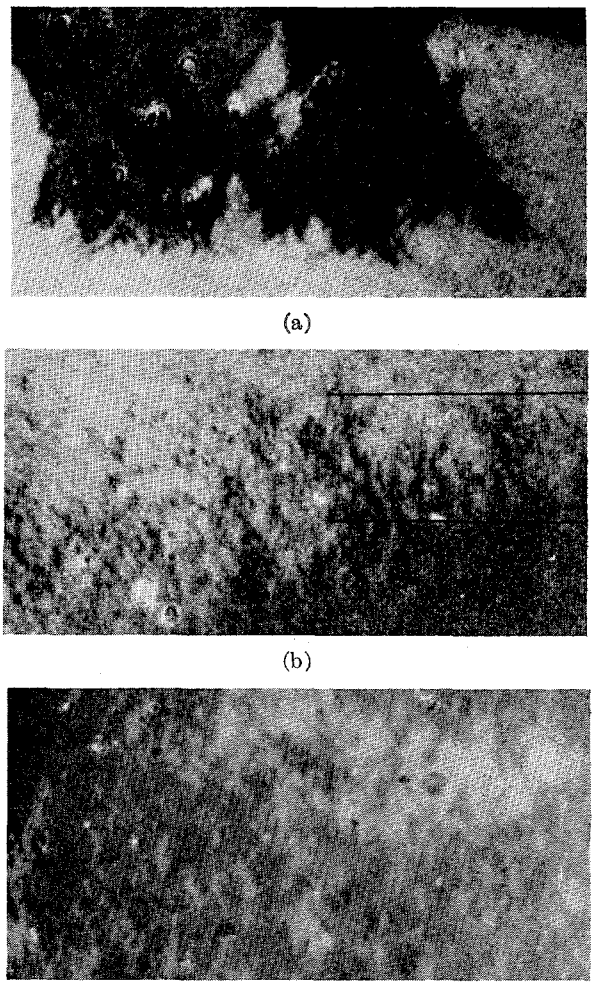

Fig. 2. (a) Highly magnified photograph of rectangular region of Fig. 1(a). (b) Highly magnified photograph of rectangular region of Fig. 1(b). Boundary width as defined by two lines is about 1.5 mm. (c) Highly magnified photograph of rectangular region of Fig. 1(c).

magnetization, but actually nucleate ahead of it when fields somewhat greater than H_c are applied, as in Fig. 1(b) (film B, H = 4.7 Oe). This may be more clearly seen in Fig. 2(b), which is a highly magnified photograph of the region within the rectangle of Fig. 1(b). Unconnected partially reversed areas of various shades of gray (indicating various amounts of rotation) are scattered throughout the boundary transition region. Again, they are poorly defined, indicating a gradual turning of the magnetization.

The unconnected areas appear over all the film when the applied field is large, as in Figs. 1(c) and 2(c) (film A, H = 5.2 Oe). Again, the areas are not well defined or regular in shape. The threshold field H_n at which the nucleation occurs over all the film is relatively well defined, as pointed out previously [2], and corresponds roughly to the start of the linear portion of a plot of the reciprocal of the switching time versus applied field [3]. The actual process of nucleation and the reason H_n is observed to be greater than H_k is not well understood. Kryder and Humphrey [3] previously showed that, with small transverse fields, nucleation occurred after the formation of a striped magnetization configuration arising from ripple. They could not observe stripes without a transverse component of applied field; a condition consistent with their use of the longitudinal Kerr effect since the longitudinal component of magnetization is the same in alternate stripes. Recently, Durasova *et al.* [6], using a stroboscopic electron microscope, have observed a striped configuration even with zero transverse field. This striped configuration should produce magnetostatic stray fields sufficiently large to prevent the rotation of the magnetization and account for the fact that $H_n > H_k$.

The diffuse boundaries are dynamic in nature but a series of photographs like those in [2, fig. 1] show that they do obtain an equilibrium width, velocity, and structure about 200 ns after application of a pulse field. Similarly, when the applied field is suddenly removed from a film, about 200 ns is required before the boundary coalesces into a well-defined narrow and jagged boundary at static equilibrium.

Boundary Width

Diffuse boundary transition width as a function of applied field shows a definite increase with increasing field, as may be seen from the experimental data shown in Fig. 3 for films B and D. The applied field in these plots is normalized with respect to the threshold field H_n, and

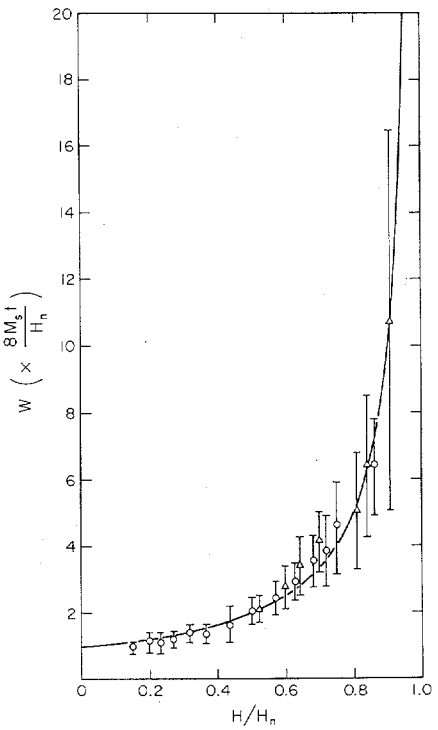

Fig. 3. Plot of boundary width as a function of longitudinal pulse field for films D (○ in center of indicated range, 8 $M_s t/H_n$ = 510 μm) and B (△ in center of indicated range, 8 $M_s t/H_n$ = 118 μm). Solid curve—prediction of (1).

the width is given in units of 8 $M_s t/H_n$ (M_s is saturation magnetization). The error bars indicate the limits of widths observed in different regions of the films. These data were taken from photographs like those in Fig. 2, and the boundary width was defined as the distance between the totally reversed magnetization and the nonreversed magnetization. For example, in Fig. 2(b), film B has an indicated boundary transition region width of 1.5 mm (= 12.5 × 8 $M_s t/H_n$) with a 4.7-Oe applied field (H/H_n = 0.9).

The solid line of Fig. 3 represents values estimated from a simple line-charge model of the boundary. This model is based on the observations (from photographs like those in Fig. 2) that the boundary transition region consists of nucleated regions of reversed and partially reversed magnetization, and that a given film has a relatively well-defined threshold H_n at which this nucleation occurs. To estimate the transition width the distance in which the applied field plus the magnetostatic stray fields drop to below the nucleation threshold was calculated. At the leading edge of the boundary the stray fields were approximated by the field from a line charge of 2 $M_s t$ located at the center of the transition region. The total field H_T a distance x from the center is then $H_T = H + 4\ M_s t/x$, where H is the applied field. Setting $H_T = H_n$, the width W is given by

$$W = 2\,x\big|_{H_T = H_n} = \frac{8M_s t}{H_n}\,\frac{1}{1 - H/H_n}. \qquad (1)$$

The fit of (1) to the experimental data is shown to be good over a relatively wide range of applied field (0.15 H_n to H_n) in Fig. 3. Presumably, the large variation in widths measured for fields slightly less than H_n is due to variations in H_n as a function of position in the film. This view is supported by the fact that boundaries in some specific geometric regions of the film are consistently at the high end of the variation of widths indicated in Fig. 3, while the boundaries in other regions are consistently at the low end. This line-charge model accurately predicts not only the dependence of the boundary width on applied field, but also the proper linear dependence on film thickness. This may be verified in part from the data of Fig. 3, where the data of both 3500- and 960-Å thick films fit the theoretical curve when the films' respective values of 8 $M_s t/H_n$ are used for the vertical scale factor. Other data (not shown) taken for films A and C indicate that the linear thickness dependence of (1) holds throughout the 500–3500-Å range.

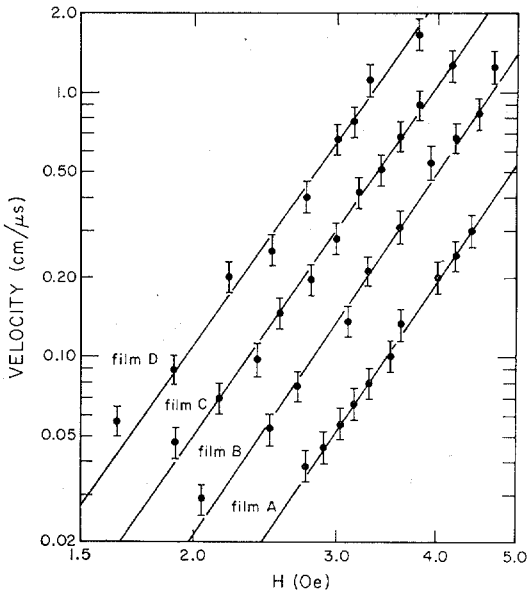

Fig. 4. Plot of boundary velocity versus applied field for four films of different thicknesses. Horizontal log scale is expanded 3.2 times with respect to vertical.

Boundary Velocity

A rapid increase in diffuse boundary propagation velocity with increasing field was previously reported [2]. The log of the velocity v is plotted in Fig. 4 as a function of the log of the applied field H for each film of Table I, the velocity measurement is estimated to be accurate to about ±15 percent, as is indicated by the error bars on the plot. The data for each film lies on a different line, which has a slope of about 5, indicating $v \propto H^{\approx 5}$. The data for each film is shifted from that of the others and indicates an approximately linear dependence on thickness.

The velocity of a moving boundary may be calculated by dividing its width by the time it takes the average magnetization within the boundary to reverse. The average reversal time for the magnetization within the diffuse boundaries may be estimated by using data for the entire film as long as it is clear that the drive field is large enough such that sequential processes play an insignificant role in

the reversal. As pointed out earlier, the nucleation process occurring in the boundary transition region appears the same as the process occurring over all the film when large fields are applied. The switching curve in the large drive field region where nucleation of reverse domains dominate the reversal process has been previously found [3], [7], [8] to be represented by

$$T^{-1} = S(H - H_0) \tag{2}$$

where T is the measured switching time, S the empirically determined switching coefficient, and H_0 an empirically determined field threshold (which is found to be less than H_n).

This empirical equation obtained from the switching curve for a film may be used to determine the average reversal time within the boundary transition region if the magnetostatic stray fields in the boundary are added to the applied field H. Although the line charge approximation used to calculate the boundary width may be used to calculate average stray fields at the transition region edge, it is not valid in the center of the transition region. However, it certainly must be possible to represent the average stray field in the transition region as $\langle H_s \rangle = CM_st/W$, where C is a dimensionless constant. The dependence must be of this form since $2\ M_st$ is the total effective magnetostatic charge and since the charge will be spread over a larger distance as W increases. In general, C could vary as W changes since the charge distribution as a function of normalized (to W) distance through the transition region could change with W. It will be shown, however, that the experimental data indicate that C is independent of boundary width or film thickness. The velocity may then be calculated from $v = WT^{-1}$ with $H + \langle H_s \rangle$ substituted for H in T^{-1}. Using (1) for W the velocity may be put into the form

$$v = S\left(\frac{H_n - H_0}{H_n}\right) WH + SM_st\left(\frac{CH_n - 8H_0}{H_n}\right). \tag{3}$$

Representative velocity data are replotted in Fig. 5 as a function of WH. The value of W was calculted from (1). The solid line represents (3) with the values of S, H_0, and C taken to make the best fit to the data. Using values of S and H_0 predicted from the switching curve [3, fig. 1] for film B and a value of C chosen for a best fit, the dashed line can be calculated. This agreement of (3) with the data, not only in form, but also in magnitude, to an accuracy of about 25 percent, clearly confirms the connection between the nucleation processes and the diffuse boundary propagation. The slight difference in slope could easily be reduced to zero by the choice of another definition for switching time since, as Humphrey and Gyorgy [7] pointed out,

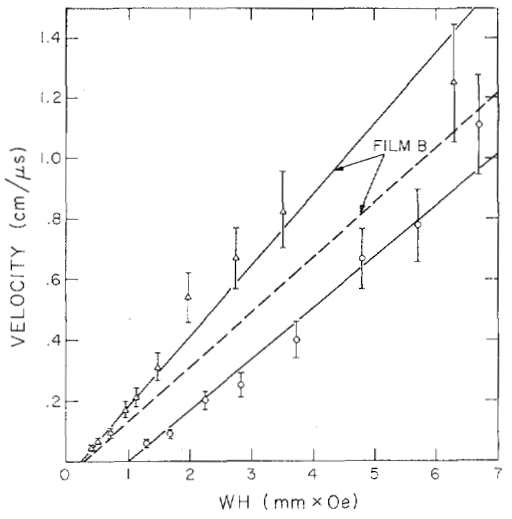

Fig. 5. Plot of boundary velocity as a function of WH for films B (Δ in center of indicated range) and D ($\bigcirc$ in center of indicated range).

slight changes in switching time definition can produce 40 percent changes in S. The observation that the velocity data also fit a relation of the form $v \propto H^{\approx 5}$ is consistent with the preceding interpretation since the scatter in the velocity measurement makes both fits possible. It can be seen, then, that (3) predicts the behavior of the diffuse boundary propagation well within the accuracy of the experiments, relates the microscopic nucleation process in the boundary to that seen in the entire film, and suggests the surprising result that the constant C is independent of width and thickness and seemingly independent of the film since all films here indicate that $C = 3.7 \pm 0.3$.

References

[1] M. H. Kryder and F. B. Humphrey, "A nanosecond Kerr magnetooptic camera," *Rev. Sci. Instrum.*, vol. 40, June 1969, pp. 829–840.

[2] ——, "Dynamic Kerr observations of high-speed flux reversal and relaxation processes in Permalloy thin films," *J. Appl. Phys.*, vol. 40, May 1969, pp. 2469–2474.

[3] ——, "Mechanisms of reversal with bias fields, deduced from dynamic magnetization configuration photographs of thin films," *J. Appl. Phys.*, vol. 41, Mar. 1970, pp. 1130–1138.

[4] ——, "Dynamic formation of diffuse boundaries and quasi-static domain growth in magnetic thin films," presented at the 4th Int. Colloq. Magnetic Thin Films, Prague, Czechoslovakia, Sept. 1970; also *Czech. J. Phys. B*, to be published.

[5] T. Suzuki, C. H. Wilts, and C. E. Patton, "Lorentz microscopy determination of domain-wall width in thick ferromagnetic films," *J. Appl. Phys.*, vol. 39, Mar. 1968, pp. 1983–1986.

[6] U. A. Durasova, I. S. Kolotov, O. S. Kolotov, V. I. Petrov, G. V. Spivak, and R. V. Telesnin, "Investigation of incoherent rotation in thin magnetic films by means of a stroboscopic electron microscope," presented at the 4th Int. Colloq. Magnetic Thin Films, Prague, Czechslovakia, Sept. 1970; also *Czech. J. Phys. B*, to be published.

[7] F. B. Humphrey and E. M. Gyorgy, *J. Appl. Phys.*, vol. 30, 1959, p. 935.

[8] C. D. Olson and A. V. Pohm, *J. Appl. Phys.*, vol. 24, 1958, p. 284.